PHYSICAL REVIEW A **85**, 062511 (2012)

First-principles molecular-dynamics simulation of biphenyl under strong laser pulses by time-dependent density-functional theory

Jun Haruyama,[*] Chunping Hu, and Kazuyuki Watanabe
Department of Physics, Tokyo University of Science, 1-3 Kagurazaka, Shinjuku-ku, Tokyo 162-8601, Japan

(Received 25 May 2012; published 21 June 2012)

The femtosecond laser reaction dynamics of the 3,5-difluoro-3′,5′-dibromo-biphenyl (DFDBrBPh) molecule is investigated using time-dependent density-functional theory combined with molecular-dynamics (TDDFT-MD) simulation. This work is based on a recent experiment that monitored torsional motion of the DFDBrBPh molecule by femtosecond time-resolved Coulomb explosion imaging [Madsen *et al.*, Phys. Rev. Lett. **102**, 073007 (2009)]. The results confirm that the probe pulse triggers a Coulomb explosion and the kick pulse induces the torsional motion of two phenyl rings, using the experimental settings of the lasers. The Coulomb explosion dynamics simulation verifies that the F and Br atoms dissociate to the ion detector while maintaining their initial alignment with respect to the phenyl rings, which is the fundamental basis of Coulomb explosion imaging of molecular torsion. Furthermore, the period and amplitude of the torsional motion obtained by the simulation are consistent with the experimental values. This validates the ability of the TDDFT-MD method to reveal the underlying mechanism of experimentally observed molecular torsional dynamics.

DOI: 10.1103/PhysRevA.85.062511 PACS number(s): 31.15.ee, 33.15.Hp, 42.50.Hz

I. INTRODUCTION

Manipulation of molecular geometry, alignment, motion, and reaction with complete control is the central aim of photophysical and photochemical scientists. Recent progress in laser technology [1,2] has made three-dimensional (3D) alignment [3,4], control of torsional or other motions [5,6], and the time-domain observation of reaction dynamics [7,8] available. In particular, the advancement of molecular alignment techniques by intense laser pulses has enabled the direct comparison of experimental and theoretical studies. Many studies have shown that strong nonresonant laser fields can effectively manipulate the external degrees of freedom of isolated gas phase molecules [9–12]. Such manipulation is dependent on the laser-induced forces and torques, which are the result of the interaction between the dipole moment and laser fields. It has been recently suggested that coherent control of molecular torsion can be realized, so that the torsional angle can be driven to an arbitrary configuration or free internal rotation can be induced by the choice of field parameters [13].

To understand the laser-molecule interaction, a reliable description of the dipole-laser interaction is necessary in the numerical calculation. To date, nonresonant reaction analysis in the literature has been restricted to a rigid rotor model under the interaction between a polarizability tensor and an electric field [13,14]. Strong laser pulses may cause structural rearrangement accompanying nonlinear effects [15]; therefore, it is important to conduct the simulation without approximations of the laser-dipole interaction. Time-dependent density-functional theory combined with molecular-dynamics (TDDFT-MD) simulation is a promising method in this respect [16], because the laser-dipole interaction is treated in a first-principles framework. Therefore, TDDFT methods can be employed to deal with highly nonlinear phenomena, such as multiphoton ionization [17,18] and harmonic generation [19,20]. However, TDDFT-MD studies are presently limited to small atomic and molecular systems due to the computational costs. Consequently, there are few studies to directly compare the time-domain observation and TDDFT-MD simulation. Thus, the objective of this paper is a quantitative comparison of experimental results and TDDFT-MD simulation to provide the basis for validation of the previous theoretical approaches [13,14].

We have focused on TDDFT-MD simulation of the laser reaction dynamics of the 3,5-difluoro-3′,5′-dibromo-biphenyl (DFDBrBPh) molecule, which was used in the experiment by Madsen and co-workers [14,21]. In their study, three laser pulses are applied to the molecule. First, a nanosecond laser pulse spatially aligns the stereogenic carbon-carbon bond axis (the molecular geometry is depicted in Fig. 1). An intense femtosecond kick pulse polarized perpendicular to the nanosecond pulse then induces torsional motion between the two phenyl rings. Lastly, a femtosecond probe pulse is used to monitor both the internal and external rotational motions of the molecule by time-resolved Coulomb explosion imaging. It is noted that the third probing process is based on the knowledge that the Br^+ and F^+ fragment ions recoil in the planes defined by the Br- and F-phenyl rings. Thus, by recording the velocities of both ion species with two-dimensional ion imaging [22], the instantaneous orientation of each of the two phenyl planes at the time of the probe pulse can be determined. From a theoretical point of view, a dynamics simulation of the three processes corresponding to the alignment, kick, and probe pulses can be carried out independently. The working mechanism of the alignment pulse has been thoroughly understood [23]; therefore, we concentrate on an investigation of the kick and probe pulses. First, the dynamical behaviors of the F and Br ions in the Coulomb explosion are studied, which is necessary to determine the working mechanism for the Coulomb explosion imaging of the experiment. A molecular torsional dynamics simulation is then conducted, from which the period and amplitude of the torsional motion can be directly obtained. It is worth

---

[*] j1210706@ed.tus.ac.jp

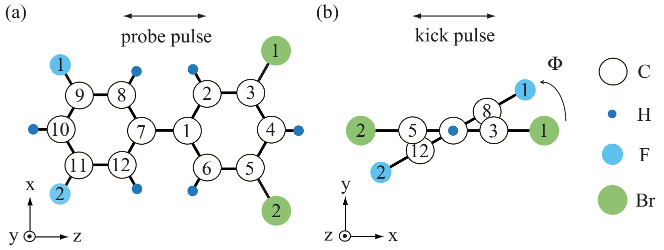

FIG. 1. (Color online) Schematic geometry of the DFDBrBPh molecule and laser polarization directions for (a) top and (b) side views. The molecule consists of a pair of phenyl rings with a torsional angle Φ between the rings around the molecular axis (the z axis). The kick and probe pulses are polarized in the x and z directions, respectively.

noting that the experiment was carried out in the gas phase, so laser fields do not interact with the medium. Therefore, an accurate reproduction of the experimental setup, such as laser intensity and wavelength, is possible. With respect to the molecular alignments, the molecular orientation technique with the nanosecond pulse enables direct comparison of the simulation with the observable torsional angles.

The remainder of this paper is organized as follows. In Sec. II, the real-space DFT method used to obtain the ground-state potential energy surfaces (PESs) and the TDDFT-MD method used to simulate the laser reaction dynamics are described. In Sec. III A, PESs for the torsional angle are given and compared with early studies. In Sec. III B, the Coulomb explosion dynamics triggered by the probe pulse are presented to demonstrate the applicability of TDDFT-MD and to validate the mechanism of Coulomb explosion imaging. In Sec. III C, the torsional dynamics induced by the kick pulse are presented and compared with the experiment. We also discuss the relevance between this work and other theoretical studies. Finally, a summary of the results and concluding remarks are given in Sec. IV.

II. METHODS AND COMPUTATIONAL DETAILS

Some technical details of the real-space DFT method used to calculate the initial ground state are briefly described. The Kohn-Sham equation is self-consistently solved using the higher-order finite-difference method [24] with a nine-point formula. The interactions between the ionic cores and the electrons are described as a norm-conserving pseudopotential, formulated by Troullier and Martins [25] based on the Kleinman-Bylander separable form [26,27]. The pseudopotential data provided by Kobayashi [28] was used in the present calculation. The exchange-correlation energy is treated within the local-density approximation (LDA) using the Ceperly-Alder functional [29] with the Perdew-Zunger parametrization [30]. The calculation box has dimensions of $12.9 \times 12.9 \times 16.7$ Å^3 with a grid spacing of 0.159 Å. The DFDBrBPh molecule is set at the center of the box and the molecular geometry is illustrated with respect to the xyz axis in Fig. 1. The DFDBrBPh molecule consists of a pair of phenyl rings with the torsional angle Φ between the rings. In this study, only the S_a enantiomer is used [31].

We now present details of the TDDFT-MD approach used for the simulation of the Coulomb explosion and molecular torsion dynamics. The main framework of this approach is similar to that for TDDFT simulation of Coulomb explosion dynamics in Ref. [32] and other incident laser reaction dynamics in the literature [33,34]. The electron system is described by the TD Kohn-Sham equation, and the ions are assumed to be classical particles moving under Hellmann-Feynman forces [35]; therefore, the TDDFT-MD simulation follows the Ehrenfest dynamics. The time-evolution operator is approximated by the fourth-order Taylor expansion [36]. The self-consistent field is treated within the second-order predictor-corrector scheme [16] and the adiabatic LDA functional is used. The laser pulse is treated as a spatially uniform electric field with a Gaussian temporal profile, which is the dipole approximation, and its functional form is given by

$$v_{\mathrm{laser}}(\boldsymbol{r},t) = \boldsymbol{r} \cdot \boldsymbol{e} E_0 \exp\left[-\frac{(t-t_0)^2}{\sigma^2}\right] \sin \omega t, \qquad (1)$$

where $\sigma = \mathrm{FWHM}/2\sqrt{\ln 2}$ is the dispersion of the laser pulse (FWHM = full width at half maximum of the pulse), t_0 is selected as 2σ, E_0 and ω are the strength and angular frequency of the electric field, respectively, and $\boldsymbol{e}$ is the unit vector of the electric field. The time step employed in the TD calculations is 4.84×10^{-4} fs. Basis sets, pseudopotentials, box size, and grid spacing are the same as those used for the DFT calculation. In the following simulations, all atom velocities are set to zero at the initial condition. Other computational details are given in a previous paper [37].

III. RESULTS

A. Potential energy surfaces

The ground-state PES of DFDBrBPh as a function of the torsional angle Φ is presented in Fig. 2(a), together with that of the BPh molecule for comparison. In this calculation, the planar structure of each phenyl ring is maintained. There have been previous studies on the torsional barrier energy of the BPh molecule, for example, Ref. [38]. The presently obtained PES quantitatively agrees with the reference; the stable angle of 39° and the torsional barrier of 0.1 eV are consistent with the quantum chemical calculation values of 39° and 0.08 eV [38]. Figure 2(b) shows the total electron density plot for the DFDBrBPh molecule. Electron polarization occurs due to the high electronegativity of F compared with that of Br, which results in a decrease of the torsional angle for DFDBrBPh from 39° to 30° [see Fig. 2(a)], due to the attractive interaction between F and Br. The polarization-induced interaction considerably changes the shape of the PES for DFDBrBPh. It is noteworthy that the strong polarization affects not only the ground-state PES, but also the torsional dynamics induced by the kick pulse, because the polarization enhances the dipole-laser interactions.

B. Coulomb explosion dynamics

The Coulomb explosion dynamics induced by the probe pulse are shown in Fig. 3. The polarization direction of the probe pulse and the atom numbering system are given in Fig. 1(a). The pulse parameters in the present simulation

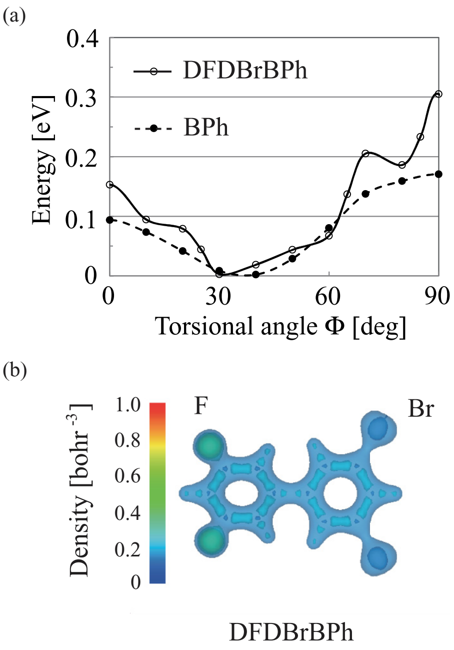

FIG. 2. (Color online) (a) Ground-state PESs as a function of the torsional angle Φ. The open circles on the solid line and the solid circles on the dashed line represent the PESs of the DFDBrBPh ($C_{12}H_6F_2Br_2$) and BPh ($C_{12}H_{10}$) molecules, respectively. (b) Total electron density plot for the DFDBrBPh molecule ($\Phi = 30°$). The DFDBrBPh molecule is strongly polarized around the F and Br atoms. The highest value of electron density is at the centers of F atoms.

(wavelength of 800 nm, pulse duration of 25 fs, and intensity of 2×10^{14} W/cm^2) are similar to the experimental values, and the corresponding electric field profile is shown in the inset of Fig. 3(a). The time evolutions of C9-F1 and C3-Br1 bond lengths are shown in Fig. 3(a), and the corresponding molecular geometries at 0 and 40 fs are presented in Fig. 3(c). When the probe pulse has peak intensity at 25 fs, the DFDBrBPh molecule gradually expands and finally dissociates. The elongation rate of the C3-Br1 bond length is less than that of the C9-F1 bond, because of the large mass of the Br atom. The behavior of the Coulomb explosion dynamics obtained in the present simulation is consistent with the experimental observation [21].

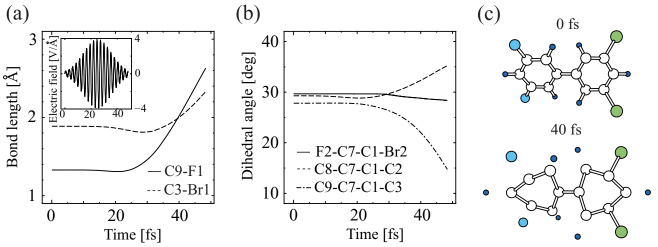

FIG. 3. (Color online) Coulomb explosion dynamics induced by the probe pulse. (a) Time evolutions of the C9-F1 (solid line) and C3-Br1 (dashed line) bond lengths. The electric field amplitude of the probe pulse is shown in the inset. (b) Time evolutions of the F2-C7-C1-Br2 (solid line), C8-C7-C1-C2 (dashed line), and C9-C7-C1-C3 (dotted dashed line) dihedral angles. (c) Molecular geometries at 0 and 40 fs. The colored (gray) ball representations are given in Fig. 1.

Furthermore, the TDDFT-MD simulation provides extra information on the detailed motion of the explosion process, in which phenyl rings are bent and deformed. Figure 3(b) shows the time evolutions of the F2-C7-C1-Br2, C8-C7-C1-C2, and C9-C7-C1-C3 angles. Here, the F2-C7-C1-Br2 dihedral angle is measured clockwise from the F2C7C1 plane to the C7C1Br2 plane. In the calculation of the dihedral angle, the initial coordinates of the C7 and C1 atoms are used to clearly indicate the motions of the F and Br atoms. In contrast, the C8-C7-C1-C2 and C9-C7-C1-C3 angles rapidly deviate from their initial values after approximately 20 fs, whereas the F2-C7-C1-Br2 angle remains almost constant around 30°. This result confirms the assumption that the F and Br atoms dissociate to the ion detector while maintaining their initial alignment. Therefore, the instantaneous orientations of each phenyl plane can be determined by recording the velocities of both ion species with TD ion imaging. The distinct behavior of the F and Br atoms with respect to C atoms indicates the necessity of using the DFDBrBPh molecule instead of the BPh molecule. The effectiveness of the femtosecond time-resolved Coulomb explosion imaging with DFDBrBPh [21] is verified by the present TDDFT-MD simulation. This is the first of two important findings in the present study.

C. Torsional dynamics induced by kick pulse

The simulated results for the torsional motion dynamics induced by the kick pulse are shown in Fig. 4. The polarization direction of the kick pulse in the simulation is illustrated in Fig. 1(b), while that in the experiment is not fixed to a single direction, because molecules in the gas phase rotate around the polarization axis of the nanosecond pulse. This is the only difference between the experimental and simulation conditions [14]. The parameters of the kick pulse (wavelength of 800 nm, pulse duration of 0.7 ps, and intensity of 5×10^{12} W/cm^2) are set according to those in the experiment, and the Gaussian envelope of the electric field is given in the inset of Fig. 4. The simulation was stopped at $t = 0.7$ ps (about 1.5×10^6 time step), because the numerical accuracy of energy conservation including work from the laser interaction [39] becomes larger than 1 eV (the relative error is 0.025%). As a common issue of TDDFT-MD, integration errors caused by a large number of operations of the time-evolution operator are unavoidable. The

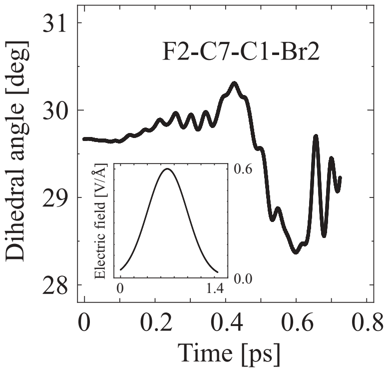

FIG. 4. Time evolution of the F2-C7-C1-Br2 dihedral angle induced by the kick pulse. The Gaussian envelope for the electric field of the kick pulse is shown in the inset.

error tends to increase when the velocities of atoms increase [40] and the difference in reaction time between atoms and electrons becomes large. However, the amount of error for the energy until 0.5 ps is still negligibly small so as to not influence the atomic motion, and thus the essence of the present results does not change.

The time evolution of the F2-C7-C1-Br2 dihedral angle is shown in Fig. 4. For a quantitative comparison of the simulation and experiment, the initial coordinates of the C7 and C1 atoms are used in the calculation of the dihedral angle to show the motions of F and Br atoms. This is because the motions of F and Br ions are recorded by the Coulomb explosion imaging experiment and not the dihedral angles. The F2-C7-C1-Br2 angle is initially 29.7°, which increases to a peak accompanied by small oscillations. The peak oscillates to a minimum, followed by further small oscillations to reach the initial value. This behavior indicates that the F2-C7-C1-Br2 oscillates with a short (about 50 fs) and a long (0.5–1.0 ps) period, as shown in the curve in Fig. 4. Although the long period is not fully reproduced due to the computational limitations, the long period of torsional motion can be estimated as 0.5–1.0 ps, which is comparable to that in the experiment. Moreover, the oscillation amplitude, 0.7°–1.0°, is in good agreement with 0.6° obtained by experiment [21]. Accordingly, the present simulation reproduced the kick-pulse-induced torsional motion of phenyl rings with similar amplitude and period as that observed in the experiment. Furthermore, the results indicate that the C-C stretching mode in the phenyl rings, which corresponds to the short period oscillations, is expected to occur in the experiments; this is the second important finding in the present study.

D. Discussion

Here, we discuss the relevance of the present simulation to previous theoretical studies. In the previous theoretical studies, the molecular torsional motion was analyzed using the quantum mechanical equation with *rigid rotor* models for the two phenyl rings in DFDBrBPh [14] and analogous molecules [13]. Madsen *et al.* [14] directly compared the theoretical and experimental results for DFDBrBPh, assuming that the full laser-dipole interactions are the same as those between the induced dipole and laser electric field in a linear regime. They interpreted the simulation results as follows. The time-varying potential, which is derived from the sum of the laser-free potential and the dipole-electric field interaction, induces torsional motion, and the oscillation period is characterized by the torsional potential and the relative moment of inertia for the two phenyl rings around the molecular axis. The present results are in good agreement with their simulation with respect to the oscillation period (about 1 ps). In addition, the initially increasing trends of the torsional angle are also in agreement, which indicates that the time-varying potential accounts for the dipole-laser interaction.

However, there are two points of note regarding the previous study reported in Ref. [14]. First, the rigid rotor models only take account of torsional motion, whereas the TDDFT-MD results for the F2-C7-C1-Br2 angle show an extra oscillation within a short period (about 50 fs), which is related to the C-C vibration mode. This indicates that the higher oscillation mode, which is not involved in the rigid rotor model, is slightly excited by the kick pulse. Second, the time-varying potential does not include nonlinear terms. Although this treatment poses little problem in the present case, a simulation that takes account of nonlinear effects would be necessary to determine if the linear response treatment is reasonable, especially under strong laser pulses. In this respect, the TDDFT-MD method is well suited for the treatment of nonlinear effects beyond the rigid rotor models.

It should be noted that the present TDDFT-MD simulation cannot treat the splitting of the nuclear wave packets at the branching of the S_a and R_a enantiomers when the torsional angle is 0°. In such cases, the TDDFT-MD simulation should take account of nonadiabatic effects [41,42]. However, as far as the motion is near the stable torsional angle, the branching problem does not need to be considered.

IV. CONCLUSION

The femtosecond laser reaction dynamics of a DFDBrBPh molecule was investigated using TDDFT-MD simulation. The results confirm that the probe pulse triggers a short-duration Coulomb explosion and the kick pulse induces torsional motion of the two phenyl rings for a long duration by selection of the laser parameters. The Coulomb explosion dynamics simulation confirms that the F and Br atoms dissociate to the ion detector while maintaining their initial alignment with respect to the phenyl rings, which is the fundamental basis for Coulomb explosion imaging of molecular torsion. The period (0.5–1 ps) and amplitude of the torsional motion (0.7°–1.0°) are consistent with experimental values reported by Madsen *et al.* [14]. Since the TDDFT-MD method takes account of the electric dipole-laser interaction without assumptions, the simulation enables quantitative understanding of laser-induced ultrafast molecular dynamics at a microscopic level.

ACKNOWLEDGMENTS

This work was supported in part by the Project of Materials Design through Computics: Complex Correlation and Non-Equilibrium Dynamics, a Grant in Aid for Scientific Research on Innovative Areas, and the Next Generation Super Computing Project, Nanoscience Program of the Ministry of Education, Culture, Sports, Science and Technology (MEXT) of Japan. K.W. acknowledges partial financial support from MEXT through a Grant-in-Aid (Grant No. 22104007). Parallelized calculations were conducted on the supercomputers of the Institute for Solid State Physics, the University of Tokyo.

[1] M. Hentschel, R. Kienberger, C. Spielmann, G. A. Reider, N. Milosevic, T. Brabec, P. B. Corkum, U. Heinzmann, M. Drescher, and F. Krausz, Nature (London) **414**, 509 (2001).

[2] M. Drescher, M. Hentschel, R. Kienberger, G. Tempea, C. Spielmann, G. A. Reider, P. B. Corkum, and F. Krausz, Science **291**, 1923 (2001).

[3] J. G. Underwood, Nat. Phys. **5**, 253 (2009).

[4] O. Ghafur, A. Rouzée, A. Gijsbertsen, W. K. Siu, S. Stolte, and M. J. J. Vrakking, Nat. Phys. **5**, 289 (2009).

[5] T. Muraoka, K. Kinbara, and T. Aida, Nature (London) **440**, 512 (2006).

[6] B. J. Sussman, D. Townsend, M. Y. Ivanov, and A. Stolow, Science **314**, 278 (2006).

[7] S. Baker, J. S. Robinson, C. A. Haworth, H. Teng, R. A. Smith, C. C. Chirilă, M. Lein, J. W. G. Tisch, and J. P. Marangos, Science **312**, 424 (2006).

[8] S. S. Viftrup, V. Kumarappan, S. Trippel, H. Stapelfeldt, E. Hamilton, and T. Seideman, Phys. Rev. Lett. **99**, 143602 (2007).

[9] H. Stapelfeldt, H. Sakai, E. Constant, and P. B. Corkum, Phys. Rev. Lett. **79**, 2787 (1997).

[10] S. Ramakrishna and T. Seideman, Phys. Rev. Lett. **99**, 103001 (2007).

[11] F. Filsinger, J. Küpper, G. Meijer, L. Holmegaard, J. H. Nielsen, I. Nevo, J. L. Hansen, and H. Stapelfeldt, J. Chem. Phys. **131**, 064309 (2009).

[12] F. Filsinger, G. Meijer, H. Stapelfeldt, H. N. Chapman, and J. Küpper, Phys. Chem. Chem. Phys. **13**, 2076 (2011).

[13] S. M. Parker, M. A. Ratner, and T. Seideman, J. Chem. Phys. **135**, 224301 (2011).

[14] C. B. Madsen, L. B. Madsen, S. S. Viftrup, M. P. Johansson, T. B. Poulsen, L. Holmegaard, V. Kumarappan, K. A. Jørgensen, and H. Stapelfeldt, J. Chem. Phys. **130**, 234310 (2009).

[15] C. A. Ullrich and A. D. Bandrauk, in *Time-Dependent Density Functional Theory*, edited by M. A. L. Marques, C. A. Ullrich, F. Nogueira, A. Rubio, K. Burke, and E. K. U. Gross (Springer, Berlin, 2006), p. 357.

[16] O. Sugino and Y. Miyamoto, Phys. Rev. B **59**, 2579 (1999).

[17] B. Walker, B. Sheehy, L. F. DiMauro, P. Agostini, K. J. Schafer, and K. C. Kulander, Phys. Rev. Lett. **73**, 1227 (1994).

[18] C. A. Ullrich, J. Mol. Struct.: THEOCHEM **501**, 315 (2000).

[19] A. L'Huillier and P. Balcou, Phys. Rev. Lett. **70**, 774 (1993).

[20] X.-M. Tong and S.-I Chu, Phys. Rev. A **64**, 013417 (2001).

[21] C. B. Madsen, L. B. Madsen, S. S. Viftrup, M. P. Johansson, T. B. Poulsen, L. Holmegaard, V. Kumarappan, K. A. Jørgensen, and H. Stapelfeldt, Phys. Rev. Lett. **102**, 073007 (2009).

[22] V. Kumarappan, C. Z. Bisgaard, S. S. Viftrup, L. Holmegaard, and H. Stapelfeldt, J. Chem. Phys. **125**, 194309 (2006).

[23] H. Stapelfeldt and T. Seideman, Rev. Mod. Phys. **75**, 543 (2003).

[24] J. R. Chelikowsky, N. Troullier, and Y. Saad, Phys. Rev. Lett. **72**, 1240 (1994).

[25] N. Troullier and J. L. Martins, Phys. Rev. B **43**, 1993 (1991).

[26] L. Kleinman and D. M. Bylander, Phys. Rev. Lett. **48**, 1425 (1982).

[27] G. B. Bachelet, D. R. Hamann, and M. Schlüter, Phys. Rev. B **26**, 4199 (1982).

[28] K. Kobayashi, Comput. Mater. Sci. **14**, 72 (1999).

[29] D. M. Ceperley and B. J. Alder, Phys. Rev. Lett. **45**, 566 (1980).

[30] J. P. Perdew and A. Zunger, Phys. Rev. B **23**, 5048 (1981).

[31] E. L. Eliel and S. H. Wilen, *Stereochemistry of Carbon Compounds* (Wiley, New York, 1994), Chap. 6, p. 156.

[32] Y. Kawashita, T. Nakatsukasa, and K. Yabana, J. Phys.: Condens. Matter **21**, 064222 (2009).

[33] J. Haruyama and K. Watanabe, e-J. Surf. Sci. Nanotechnol. **9**, 1 (2011).

[34] S. Bubin and K. Varga, J. Appl. Phys. **110**, 064905 (2011).

[35] A. Castro, M. A. L. Marques, J. A. Alonso, G. F. Bertsch, and A. Rubio, Eur. Phys. J. D **28**, 211 (2004).

[36] K. Yabana and G. F. Bertsch, Phys. Rev. B **54**, 4484 (1996).

[37] K. Taguchi, J. Haruyama, and K. Watanabe, J. Phys. Soc. Jpn. **78**, 094707 (2009).

[38] M. Johansson and J. Olsen, J. Chem. Theory Comput. **4**, 1460 (2008).

[39] Y. Miyamoto and H. Zhang, Phys. Rev. B **77**, 165123 (2008).

[40] [http://www.tddft.org].

[41] C. Hu, H. Hirai, and O. Sugino, J. Chem. Phys. **127**, 064103 (2007).

[42] H. Hirai and O. Sugino, Phys. Chem. Chem. Phys. **11**, 4570 (2009).